

1 **Protein degradation analysis by affinity microfluidics**

2
3 Lev Brio^{1,2}, Danit Wasserman^{1,2}, Efrat Michaely-Barbiro¹, Doron Gerber^{1,3,*}, and Amit

4 Tzur^{1,3,*}

5
6 ¹The Mina & Everard Goodman Faculty of Life Sciences and the Institute for
7 Nanotechnology and Advanced Materials, Bar Ilan University, Ramat Gan, Israel.

8 ²These authors contributed equally to this work

9 ³These authors jointly supervised this work

10 * Corresponding authors

11
12 Correspondence should be addressed to amit.tzur@biu.ac.il (A.T); doron.gerber@biu.ac.il

13 (D.G)

14 Keywords: Integrated microfluidics, Protein array, Protein chip, Protein degradation,

15 Ubiquitin-proteasome, Cell cycle, APC/C, Cell-free system

16

17 **Abstract**

18 Protein degradation mediated by the ubiquitin-proteasome pathway regulates
19 signaling events in all eukaryotic cells, with implications in pathological conditions such as
20 cancer and neurodegenerative diseases. Detection of protein degradation is an elementary
21 need in basic and translational research. In vitro degradation assays, in particular, have been
22 instrumental in the understanding of how cell proliferation and other fundamental cellular
23 processes are regulated. These assays are direct, quantitative and highly informative but also
24 laborious, typically relying on low-throughput polyacrylamide gel-electrophoresis followed
25 by autoradiography or immunoblotting. We present protein degradation on chip (pDOC), a
26 MITOMI-based integrated microfluidic device for discovery and analysis of ubiquitin-
27 mediated proteolysis. The platform accommodates microchambers on which protein
28 degradation is assayed quickly and simultaneously in physiologically relevant environments,
29 using minute amount of reagents. Essentially, pDOC provides a multiplexed, sensitive and
30 colorimetric alternative to the conventional degradation assays, with relevance to biomedical
31 and translational research.

32

33

34 **Introduction**

35 Protein degradation by the ubiquitin-proteasome system is a central regulatory
36 module through which the level of proteins in all eukaryotic cells remains balanced.
37 Deviation from the desired amount of each protein at any given moment can be detrimental to
38 the cell, leading to dysfunctional tissues and a wide range of illnesses in human, including
39 cancer, cystic fibrosis, and neurodegenerative diseases [1] [2].

40 The core cascade underlying ubiquitination involves three enzymes: The E1 enzyme
41 covalently binds and activates the ubiquitin molecule for transfer to an E2 conjugating
42 enzyme. Then, the ubiquitin-conjugated E2 interacts with an E3 ubiquitin-ligase enzyme,
43 which catalyzes the transfer of ubiquitin molecules from the E2 to the target protein or to a
44 second ubiquitin molecule, typically via an isopeptide bond to a lysine residue. Finally, a
45 target protein that is covalently bound to a chain of ubiquitin moieties can be recognized by
46 the proteasome for degradation [1, 2]. Hundreds of different E3 enzymes underlie
47 the enormous functional reach and specificity of the entire ubiquitination process. With
48 respect to cell proliferation and cell cycle regulation, the ubiquitin ligases anaphase-
49 promoting complex/cyclosome (APC/C) and Skp1-Cullin-F-box protein complex (SCF) are
50 particularly important [3–5]. The substrate specificity of both complexes is dependent on co-
51 activators: Cdc20 and Cdh1 for the APC/C and one of several F-box proteins for the SCF,
52 e.g., Skp2 and β -TrCP [6–8]. Overall, orderly proteolysis mediated by cell cycle regulated E3
53 enzymes ensures unidirectional cell cycle in all eukaryotes. [6–10].

54 Protein degradation, however, cannot be automatically inferred from ubiquitination;
55 while some forms of ubiquitin chains trigger proteolysis, monoubiquitination and other forms
56 of polyubiquitination regulate signaling cascades via proteasome-independent pathways [11].
57 Furthermore, ubiquitination can be reversed by enzymes called deubiquitinases in a manner

58 that can prevent proteolysis [12]. On the flip side, proteasomal degradation may not always
59 be coupled to ubiquitination [13]. Thus, protein degradation must be determined directly.

60 Protein degradation assays in cell-free extracts, also known as ‘cell-free systems’,
61 have been instrumental in cell biology research, enabling direct and quantitative analyses of
62 ubiquitin-mediated proteolysis in physiologically relevant environments. In fact, much of the
63 cell cycle principles were discovered by monitoring the degradation of cell cycle proteins in
64 extracts from frog eggs or cycling human cells (see for example [14–20]). The extensive use
65 of these ‘degradation assays’ in today’s modern era, is a testament to their efficacy (see for
66 example [21–23]). Interestingly, conventional degradation assays have never truly benefited
67 from modern technologies, and still typically rely on gel-electrophoresis, autoradiography
68 and large amount of biological material.

69 Integrated microfluidics and pneumatic microvalves paved the way to protein chips in
70 which the arrayed proteins are freshly expressed in a physiological environment that maintain
71 proper protein folding and activity [24]. The target proteins are expressed either on chip or
72 externally, and subsequently immobilized to microchambers via a designated surface
73 chemistry. Then, a large panel of direct colorimetric assays can be performed over thousands
74 of microchambers, using minute amounts of reagents. In recent years, we developed several
75 microfluidic devices based on mechanically induced trapping of molecular interactions
76 (MITOMI), with which we discovered and detected i) protein interactions with DNA, RNA,
77 proteins and viruses; and ii) protein post-translational modification (PTM), specifically,
78 phosphorylation, autophosphorylation and ubiquitination [24–30].

79 The combination of integrated microfluidics, protein arrays and cell-free systems
80 from healthy or pathological sources holds great potential in biomedical research and
81 diagnostics. In this study, we utilize the MITOMI platform for protein degradation analyses.
82 The proof of concept is demonstrated using cell extracts with APC/C-specific activity. The

83 method, named pDOC (protein degradation on chip) provides a fast, sensitive and cost-
84 effective alternative to the classic method by which proteasome-mediated proteolysis has
85 been assayed in vitro almost unvaryingly for nearly half a century.

86

87 **Materials and methods**

88 *Plasmids*

89 pCS2-Flag-FA vector was generated by annealing Flag tag oligos and ligating final
90 fragment into pCS2-FA vector using BamHI and FseI restriction sites. pCS2-Flag-FA-
91 Securin-GFP w.t and $\Delta 64$ variant plasmids were generated by cloning w.t or $\Delta 64$ Securin-
92 GFP [27] into pCS2-Flag-FA vector, using FseI (5') and AscI (3') flanked primers. pCS2-
93 Geminin $\Delta 27$ -GFP was generated by deleting amino acids 1-27 from Geminin-GFP [27] using
94 QuikChange® Lightning mutagenesis kit (Agilent, 210513). The plasmids pCS2-Flag-FA-
95 Geminin-GFP w.t and $\Delta 27$ variant were generated by cloning Geminin-GFP into pCS2-Flag-
96 FA vector using FseI and AscI restriction sites. pCS2-Flag-FA-p27-GFP was generated by
97 replacing Geminin open reading frame (ORF) with p27 ORF using FseI and AgeI restriction
98 sites and pCS2-FA-p27 as a template [27]. Flag-p27-myc fragment was generated by a two-
99 step assembly PCR using pCS2-Flag-FA-p27-GFP template, a first primer set containing a c-
100 Flag tag (5') and a Myc tag (3'), and a second primer set containing a T7 promoter (5') and a
101 T7 terminator sequence (3'). All GFP-tagged proteins carried enhanced variant of GFP
102 (eGFP).

103 *Cell culture maintenance*

104 NDB cells are based on the HEK293 cell line. A detailed description of this cell
105 system can be found in Ref [18]. NDB and HeLa S3 (ATCC; #CCL-2.2) cells were
106 maintained in tissue culture dishes containing Dulbecco's Modified Eagles Medium
107 (DMEM) supplemented with 10% fetal bovine serum, 2 mM L-glutamine, and 1%

108 Penicillin–Streptomycin solution (Biological Industries; #01-055-1A, #04-001-1A, #03-020-
109 1B, #03-031-1B). Cells were maintained at 37°C in a humidified 5% CO₂-containing
110 atmosphere. HeLa S3 cells were either cultured on dishes or in 1-l glass spinner flasks in
111 suspension (80 rpm). NDB cells were cultured in the presence of 5µg/ml Blasticidin (Life
112 Technologies; #A11139-03) to maintain the pcDNA6/TR plasmid carrying the ORF for Tet
113 repressor.

114 *Cell synchronization*

115 For late-mitosis synchronization, NDB cells were cultured in 150 mm/diameter
116 dishes. After reaching a confluency of about 75%, the cells were treated with 1 µg/ml
117 Tetracycline (Sigma-Aldrich; #87128) for 22 hr and harvest for extract preparation. For S-
118 phase synchronization, HeLa S3 cells were cultured in suspension for 72 h up to a
119 concentration of approximately 5×10⁵ cells/ml. Cells were then supplemented with 2 mM
120 Thymidine for 22 hr, washed with DMEM (twice, 5 min, 250×g) and released into pre-
121 warmed fresh media (37°C) for additional 9 hr. Cell culture was then supplemented again
122 with 2 mM Thymidine for 19 h before harvest for extract preparation.

123 *Preparation of cell extracts*

124 HeLa S3 extracts: S-phase Synchronous HeLa S3 cells were washed with ice-cold 1×
125 PBS and lysed in a swelling buffer (20 mM HEPES, pH 7.5, 2 mM MgCl₂, 5 mM KCl, 1
126 mM Dithiothreitol [DTT], and protease inhibitor cocktail [Roche; #11836170001])
127 supplemented with energy-regenerating mixture, E-mix (1 mM ATP, 0.1 mM ethylene
128 glycol-bis [β-aminoethyl ether]-N,N,N',N'-tetra acetic acid [EGTA], 1 mM MgCl₂, 7.5 mM
129 creatine phosphate, 50 µg/ml creatine phosphokinase). Cells were incubated on ice for 30 min
130 and homogenized by freeze–thawing cycles in liquid nitrogen and passed through a 21-G
131 needle for 10 times. Extracts were cleared by subsequent centrifugation (17,000 × g; 10 and
132 40 min), and stored at –80°C. NDB mitotic extracts: Tet-induced NDB cells were collected

133 from 20-24 150 mm dishes by gentle wash with ice-cold PBS. Extracts were prepared as
134 described for HeLa S3. For more details see [18][31].

135 *In vitro expression of target proteins*

136 Target proteins were *in-vitro* expressed using rabbit reticulocyte lysate (TNT-coupled
137 reticulocyte system; Promega; #L4600, #L4610) supplemented with either ³⁵S-methionine/S-
138 L-cysteine mix (PerkinElmer; #NEG772002MC) for radiography detection or with untagged
139 Methionine (Promega #L118A) and Green Lysine (FluoroTect™ GreenLys, Promega
140 #L5001).

141 *Off-chip Degradation Assay*

142 Degradation assays were performed in 20 µl cell extract supplemented with 1 µl of
143 20× energy regenerating mixture (see above), 1 µl of 10 mg/ml Ub solution (Boston
144 Biochem; #U-100H), and 1µl radiolabeled *in vitro* translated protein of interest. For a
145 negative control, reaction mixture was supplemented with proteasome inhibitor MG132 (20
146 µM; Boston Biochem; #I-130). Reaction mixtures were incubated at 28°C, and samples of 4-
147 5 µl were collected in 15-20 min intervals. **Off-chip detection:** Time-point samples were
148 mixed with 4× Laemmli Sample Buffer (BIO-RAD #1610747), denatured (10 min, 95°C),
149 and resolved by SDS-PAGE. Gels were soaked in a Methanol/Acetic acid (10/7.5%) fixative
150 solution for 20 min, dried in vacuum and heat, and exposed to phosphor screen (Fuji) for 24-
151 72 hr. *In vitro* translated proteins were visualized by autoradiography using Typhoon FLA
152 9500 Phosphorimager (GE Healthcare Life Sciences). Signal intensity (corrected for
153 background signal) was measured by ImageJ software and was normalized to the signal at t_0 .
154 All plots were created using Microsoft Excel software, version 16.20. Mean and SE values
155 were calculated from three or four independent degradation assays. **On-chip detection:**
156 Time-point samples were immediately frozen in liquid nitrogen. Before detection, samples
157 were thawed on ice, flown through the chip for 3-5 min, and immobilized to protein

158 chambers under the ‘button’ valve (see ‘Surface chemistry’ below). Next, the ‘button’ valves
159 were closed, allowing unbound material to be washed by PBS. The level of target proteins
160 (before and after degradation reactions) were determined by 488 nm-excitation and an 535/25
161 nm emission filter. Protein level could also be measured by immunofluorescence using
162 fluorescently labeled antibodies (anti-Flag-Alexa 647, #15009; Cell Signaling, Danvers, MA,
163 USA). These antibodies were flowed into the device and incubated with the immobilized
164 proteins under the ‘button’ for 20 min at RT. Unbound antibodies were mechanically washed
165 by PBS following the closing of the ‘button’ valve. Here, target protein levels were
166 determined by 633 nm-excitation and an 692/40 nm emission filter.

167 ***Device fabrication***

168 The microfluidic device is made of two layers of PDMS. The silicon wafers are
169 written by photolithography (Heidelberg MLA 150). Then after, the soft lithography phase is
170 induced using silicon elastomer polydimethylsiloxane (PDMS, SYLGARD 184, Dow
171 Corning, USA) and its curing agent to fabricate the microfluidic devices. The microfluidic
172 devices are consisting of two aligned PDMS layers, the flow and the control layers which are
173 prepared using different ratios of PDMS and its curing agent; 5:1 and 20:1 for the control and
174 flow layers, respectively. The control layer is degassed and baked for 30 min at 80°C. The
175 flow layer is initially spin coated (Laurell, USA) at 2000 rpm for 60 sec and baked at 80°C
176 for 30 min. Next, the flow and control layers are aligned using an automatic aligner machine
177 (custom made) under a stereoscope and baked for 1.5h at 80°C for final bonding. The two-
178 layer device is then peeled off from the wafer and bound to a cover slip glass via plasma
179 treatment (air ,30%, 30 sec).

180 ***Surface chemistry***

181 Biotinylated-BSA (1 µg/µl, Thermo) is flowed for 25 min through the device,
182 allowing its binding to the epoxy surface. On top of the biotinylated-BSA, 0.5 µg/µl of

183 Neutravidin (Pierce, Rockford, IL) is added (flow for 20 min). The ‘button’ valve is then
184 closed, and biotinylated-PEG (1 $\mu\text{g}/\mu\text{l}$, (PG2-AMBN-5k, Nanocs Inc.) is flowed over for 20
185 min, passivating the flow layer, except for the buttons area. Following passivation, the
186 ‘button’ valve is released and a flow of 0.2 $\mu\text{g}/\mu\text{l}$ biotinylated anti-GFP antibodies (Abcam;
187 #ab6658, Cambridge, United Kingdom) or 0.01 $\mu\text{g}/\mu\text{l}$ biotinylated anti-Flag antibodies (Cell
188 Signaling; #2908S Danvers, MA, USA) were applied. The antibodies bound to the exposed
189 Neutravidin, specifically to the area under the ‘button’, creating an array of anti-GFP - or
190 anti-Flag tag. PBS buffer was used for washing in between steps. In the case of p27
191 immobilization, surface chemistry was performed with 0.2 $\mu\text{g}/\text{ml}$ donkey anti-mouse whole
192 IgG antibodies (#715-065-150, Jackson Immuno research laboratories, Maryland, USA)
193 followed by 20 min flow of 6.5 $\mu\text{g}/\text{ml}$ anti p27 antibodies (Santa Cruz biotechnology,
194 Heidelberg Germany; #1641 mouse).

195 ***On-chip degradation assay***

196 Flag-Securin-GFP (w.t and $\Delta 64$ mut) and p27-GFP IVT products were flowed into the
197 chip and immobilized on the surface under the ‘button’ at the protein chambers via its GFP
198 tag, following by PBS buffer wash and scanned. Next, the ‘button’ valves were opened and
199 the extract reaction mixtures were incubated with the protein chambers for 60 min (30°C).
200 During the reaction, the level of the remaining target protein was determined by GFP signal
201 every 15 min. The decline in GFP signal correlated with degradation. After background
202 signal subtraction, GFP signals were normalized to the signal at t_0 (value of 1) or between 1
203 (max signal) and 0 (min signal).

204 ***Image and data analysis***

205 LS reloaded microarray scanner, GenePix7.0 (Molecular Devices) and ImageJ image
206 analysis software were used for analysis and presentation of the images. The signal measured
207 around the button valve was considered as the background, since no immobilization of

208 proteins was expected there. Yet, some background signal is always detected, which results
209 from non-specific attachment of antibodies to the device surface. We subtracted the
210 background signal around the buttons in a ring the size of 2R with 2-pixel spacing (see
211 supplementary material in [27]).

212 ***Immunoblotting***

213 Protein samples were mixed with x4 Laemmli buffer, denatured (10 min, 96°C), and
214 resolved on freshly made 10% acrylamide gel using a Tris-glycine running buffer. Proteins
215 were then electro-transferred onto a nitrocellulose membrane (Bio-Rad; #162-0115) using
216 Trans-Blot Turbo transfer system (Bio-Rad). Ponceau S Solution (Sigma-Aldrich; #81462)
217 was used to verify transfer quality. Membrane was washed (TBS), blocked (5% skimmed
218 milk in TBST), and incubated (RT, 1 hr) with antibody solution (2.5% BSA and 0.05%
219 sodium azide in PBS) before blotted with anti-Securin (Abcam; #AB3305) primary antibody
220 (RT, 2 hrs). Anti-mouse Horseradish peroxidase–conjugated secondary antibody was
221 purchased from Jackson ImmunoResearch (#115-035-003). ECL Signal was detected using
222 EZ-ECL (Biological Industries; #20-500-171).

223

224 **Results**

225 pDOC is based on a MITOMI device, an integrated microfluidic chip originally
226 developed to quantify protein-ligand interactions at equilibrium [24, 32]. The basic design
227 was modified to contain an array of 32 by 32 microcompartments. Each compartment is
228 separated into two chambers and controlled by three valves: a ‘neck’ valve that controls the
229 diffusion (mixing) of material from chamber I into the ‘Protein chamber’, in which a specific
230 target protein is trapped; a ‘sandwich’ valve that separates between cell unites; and the
231 MITOMI ‘button’ valve, which traps interacting molecules beneath it, thus taking a snapshot
232 of the interaction at equilibrium (Figure 1A). The pDOC chip design includes separation of

233 the master control of the three valves into sections of the chip that can be activated and
234 controlled independently. Compared to the control of each valve type for the entire chip, this
235 separation not only improves valve response, but more importantly, it permits time-response
236 assays on chip. Within each section, experiments are performed in all cell units in parallel,
237 enabling high-throughput applications of the kind shown in our previous devices [24–26, 33].

238 Similar to the classic degradation assays, target proteins for pDOC analyses are in
239 vitro translated (IVT) using rabbit reticulocyte lysate that allows correct folding and PTM.
240 However, quantitative detection is based on fluorescence rather than radioactivity. The IVT
241 products are immobilized on the glass surface of the chip via biotin-avidin binding. To this
242 end, specific biotinylated antibodies are applied under the button valve. Following pull down
243 of the target protein the unbound material, such as reticulocyte lysate and cell extract, is
244 washed away. Then the entire chip is passivated by PEG-Biotin, except for the area beneath
245 the button (Figure. 1A; for more details, see our previous publications [25, 26, 33]. The
246 freedom to control flow in individual sections enables multiple regimes of surface chemistry
247 on one chip.

248 The device is compatible with multiple strategies of surface chemistry and possible
249 experimental setups (illustrated in Figure 1B): i) The target protein is tagged on both N' and
250 C' termini. One tag is used for immobilization via tag-specific biotinylated antibodies and the
251 second tag is green fluorescent protein (GFP), which is used for detection. ii) The target
252 protein is single-tagged with GFP, which is used for both immobilization and detection. iii)
253 The target protein is double tagged. Here, however, detection is based on fluorescently
254 labeled antibodies against short non-fluorescent tags (e.g., Flag). iv) The target protein is in
255 vitro translated in lysate containing fluorescent lysine and immobilized by protein-specific
256 antibodies. Importantly, immobilization can be performed with non-biotinylated antibodies if

257 the surface chemistry also includes biotinylated IgG. Overall, the flexibility of the method
258 simplifies assay optimization according to specific needs and limitations.

259

260 **pDOC facilitates analysis of protein degradation in cell-free extracts**

261 Conceptually, analysis of protein degradation by pDOC is direct, simple and fast;
262 signal detection is based on in situ quantification of fluorescent signals, thus obviating gel-
263 electrophoresis and any other gel-related procedures, e.g fixation, drying, autoradiography or
264 immunoblotting, and long exposures. pDOC functions like a chromatography column; it
265 isolates and concentrates the target protein on the protein chamber of each cell unit. Our first
266 goal was to examine whether the signal sensitivity and dynamic range of pDOC enables time-
267 based quantification of IVT products following incubation with cell extracts in tube. As a
268 proof of concept, we utilized mitotic extracts from HEK293 cells that are blocked in an
269 anaphase-like state due to high levels of non-degradable Cyclin-B1. This mitotic cell-free
270 system, hereafter referred to as NDB, recapitulates APC/C^{Cdc20}-mediated proteolysis of the
271 cell cycle proteins Securin and Geminin [18, 31].

272 Conventional degradation assays of radiolabeled Flag-Securin-GFP and Flag-
273 Geminin-GFP (IVT products) in NDB mitotic extracts are shown in Figure 2A. Control
274 experiments with non-degradable mutant variants (Geminin Δ 27 and Securin Δ 64)
275 demonstrate the specificity of the assay. Equivalent experiments were performed with non-
276 radioactive IVT products. First, we performed an end-point assay. After 60 min incubation,
277 reaction samples were loaded on pDOC through separate channels and scanned for GFP
278 fluorescence. Control reactions, in which IVT products were incubated in PBS, allowed us to
279 normalize the level of each target protein at $t_{60 \text{ min}}$ (extracts/PBS ratio) and to estimate
280 background signals. Overall, on-chip detection demonstrates a sharp reduction in the level of
281 Geminin and Securin following incubation in NDB mitotic extracts, whereas non-degradable

282 variants remained stable, exhibiting ~80% of the control GFP signals in PBS. At this
283 juncture, we noted that background signals from reticulocyte lysate, cell extracts, and non-
284 specific immobilization were minor (Figure S1).

285 Next, we tested whether pDOC can be utilized to obtain reliable kinetic information
286 on protein degradation. Flag-Securin-GFP and Flag-Geminin-GFP were incubated in NDB
287 mitotic extracts for 60 min, and reaction samples were snap frozen in liquid nitrogen every 15
288 min. After quick thawing, samples representing five time-points were loaded on the chip for
289 signal quantification. Comparable analyses were performed using SDS-PAGE and
290 autoradiography. Non-degradable Flag-Securin Δ 64-GFP and Flag-Geminin Δ 27-GFP variants
291 were also assayed by autoradiography for control. Considering the vast differences between
292 the two methods of detections, GFP and autoradiography signals were normalized between 0
293 and 1, meaning that the signal at $t_{60 \text{ min}}$ was subtracted from all other time points. The
294 resulting values were normalized to max signal at t_0 and plotted. As shown in Figure 1C and
295 D, on-chip analysis by pDOC and off-chip analysis by SDS-PAGE-autoradiography
296 exhibited near identical degradation patterns of Flag-Securin-GFP and Flag-Geminin-GFP.
297 Note that reaction cocktails contained 1 μ l IVT, 20 μ l extracts and 2 μ l ubiquitin/E. mix
298 solution, following our standard protocol [18, 27, 34] For each time point, 5 μ l reaction mixes
299 were flowed for a period of 3 min through protein chambers with open MITOMI button
300 valves, allowing immobilization of the target protein, while the neck valves were closed. This
301 loading protocol enabled clear visualization of the target protein without the concern of signal
302 saturation (Figure S2). We concluded that pDOC facilitates both end-point and time-course
303 analyses of protein degradation in vitro.

304 Importantly, Flag-Securin-GFP was immobilized to protein chambers via biotinylated
305 anti-GFP antibodies rather than anti-Flag antibodies. By doing so, we effectively
306 demonstrated that GFP can serve for both immobilization and detection, eliminating the need

307 for two tags. Overall, we find GFP to be an optimal tag for signal detection on-chip. The
308 fusion of a fluorescent protein to a target protein, however, may distort protein folding in
309 ways that effectively limit ubiquitination and proteolysis. In this context, the flexibility of
310 pDOC is particularly advantageous. Figure 3A depicts three configurations by which Securin
311 degradation was analyzed on chip. Securin level was measured at t_0 and $t_{60 \text{ min}}$. Signal
312 detection can be direct, either by GFP or green-Lys. While the former is brighter, the latter
313 allows quantification without tagging. Indirect detection by immunofluorescence was found
314 to be equally informative. Here, short immunodetectable tags minimize the risk of misfolding,
315 but the target proteins must be double tagged because a single tag cannot be used for both
316 immunolabeling and immobilization. Detection by immunofluorescence requires an
317 additional 30 min but we benefit from the bright signal of the fluorophores to which plenty of
318 commercial antibodies are coupled. All three detection protocols revealed the degradation of
319 Securin in NDB mitotic extracts.

320 The versatility of pDOC was further demonstrated using tag-free p27 (Figure 3B).
321 Degradation of p27 is mediated by SCF^{Skp2} E3 ligase, rather than APC/C, and is orchestrated
322 with the DNA synthesis (S) phase of the cell cycle [35]. p27 degradation was assayed in
323 extracts from S-phase synchronous HeLa S3 cells and analyzed by pDOC. The protein was
324 immobilized via anti-p27 and biotinylated anti-IgG antibodies, and detected by green-Lys.
325 Analysis by pDOC revealed the stereotypical instability of p27 in S-phase extracts (Figure
326 3B). The degradation pattern resembled that measured by autoradiography (Figure S3). Thus,
327 pDOC can be utilized for degradation assays of untagged proteins. Furthermore, the method
328 is specific and not restricted to a certain type of cell-free systems.

329 The advantages of autoradiography-based degradation assays include minimal signal-
330 to-noise ratio, high specificity of the signal and linearity of the assay. However, this does not
331 come without a cost. First, the ³⁵S isotope is a short-lived reagent with half-life of ~3 months.

332 Second, on the gel the signal is spread over a well of 4-5 mm width (standard 10-well gel).
333 Third, in a standard degradation assay, 1-2 μ l IVT product is diluted in 20-30 μ l cell extracts
334 whose protein concentration is about 20-25 mg/ml. Thus, the amount of IVT loaded per lane
335 is limited by the maximum separation capacity of the gel. De facto, we load 4-5 μ l of reaction
336 mix into a well of a standard 10-well mini-gel of 1 mm thick. Fourth, in vitro translation is
337 challenging for large proteins because of ribosome processivity. Thus, although large proteins
338 incorporate more radiolabeled Methionine/Cysteine relative to small proteins, the overall
339 signal of the full-length protein can be impractical for reliable quantification. Fifth, the
340 exposure time for a high-quality signal is typically within a range of 12-24 hrs. Note that the
341 abovementioned points 2-4 are equally relevant when protein degradation is assayed by SDS-
342 PAGE and immunoblotting. As for point 5, western blotting does not require long exposures.
343 Yet, the overall incubation time with antibodies is long. Furthermore, IVT products in
344 immunoblot-based assays must be tagged in order to be distinguished from the endogenous
345 proteins in the extracts. At this juncture, it is important to note that whether degradation is
346 assayed by autoradiography or immunoblotting, informative expression of IVT products must
347 be validated beforehand, in itself, a day long procedure. Equivalent validation by pDOC is
348 instantaneous.

349 On-chip, the fluorescence signals of Flag-Securin-GFP at $t_{60 \text{ min}}$ were above
350 background level and more noticeable compared to autoradiography (Figures 2A, 3A and
351 S1). Yet, when the signal at $t_{60 \text{ min}}$ was subtracted from all other time-points, the overall
352 degradation patterns of Flag-Securin-GFP, as revealed by pDOC and autoradiography, was
353 similar (Figure 2C and D). This observation suggests that pDOC detects protein residue still
354 lingering in the reaction mix after 60 min incubation, and which are barely detected by
355 autoradiography, if at all. Thus, it can be argued that the sensitivity of pDOC surpasses that
356 of the conventional autoradiography, and if so, pDOC not only facilitates in vitro degradation

357 assays, but also significantly reduces reagent consumption and cost per assay. To test that, we
358 diluted Flag-Securin-GFP in reticulocyte lysate 4- and 10-fold and incubated the substrate in
359 NDB mitotic extracts for 1 hr, while maintaining the original reticulocyte lysate /extract
360 volume ratio of 1/20 (μ l). Time point samples were analyzed by pDOC (based on GFP
361 fluorescence). Equivalent experiments performed in parallel with 35 S-labeled Flag-Securin-
362 GFP, following the conventional assay. To clarify, radiolabeled and non-radiolabeled
363 substrates were expressed simultaneously from the same TNT®/DNA solution mix.
364 Furthermore, degradation assays performed a day after delivery of the 35 S-Met/ 35 S-Cys
365 solution to our lab (\sim 1175Ci/mmol), and the gels were exposed to phosphor screen overnight.
366 Yet, whenever the IVT substrate was diluted, the signal obtained by autoradiography was
367 below any acceptable standard, even at t_0 , and decreased to barely or undetectable levels after
368 15 min incubation (Figure 4A). Conversely, analyses by pDOC were informative in all three
369 conditions (Figure 4B). We could detect bona fide signals of 4- and 10-fold diluted Flag-
370 Securin-GFP at t_0 as well as at $t_{60 \text{ min}}$, recording the full dynamics of the protein in NDB
371 mitotic extracts. On a more practical note, we effectively demonstrated that protein
372 degradation can be analyzed with 0.1 μ l IVT product and 2 μ l cell extracts, thereby saving
373 90% of the reagents. This feature is particularly valuable in assays which rely on limited
374 biological material, e.g., extracts from primary cells, and normal/pathological tissue samples.
375 pDOC unveils remanent amount of Flag-Securin-GFP that could not be visualized by
376 conventional methods. Interestingly, while the overall degradation pattern of Flag-Securin-
377 GFP in all three conditions was similar, we noticed a systematic delay in Flag-Securin-GFP
378 degradation as the substrate concentration was reduced. This observation has not been
379 identified previously in our lab, and could be attributed to rate-limiting steps along the
380 process of ubiquitination/degradation of Securin, and perhaps APC/C substrates overall [36,

381 37]. Note that the estimated concentration of Flag-Securin-GFP in the reaction mix was 17
382 nM (before further dilution in reticulocyte lysate; Figure S4).

383

384 **On-chip assay for protein degradation**

385 Until now, we have demonstrated the capacity of pDOC to facilitate analysis of *in*
386 *tube* protein degradation assays, i.e. the assay takes place prior to its introduction to the chip
387 (Figures 2-4). However, our protocol enables a complete on-chip assay for protein
388 degradation. Reaction samples are loaded on the chip while neck-valves are closed, i.e.,
389 without access to chamber I. Target proteins are then immobilized and captured at the protein
390 chamber and remaining materials are washed away (Figure 1A). Technically, the neck valve
391 allows trapping of a target protein in the protein chamber under the MITOMI button valve,
392 and cell-free extracts in chamber I, noted here as ‘extract chamber’ (Figure 5A). The opening
393 of the neck valve enables diffusion of cell extracts into the protein chamber. The motivation
394 for an on-chip assay is threefold: 1) higher-throughput, especially if the target proteins are
395 expressed on-chip, which is possible for MITOMI-based devices; 2) reagent-saving and cost
396 per assay. In fact, 5 μ l cell extracts are sufficient to fill a thousand cell units; 3) analysis of
397 protein degradation in real time. The challenge, however, is the limited degradation capacity
398 of <1 nl extracts per cell unit, which never been tested on any platform.

399 We decided to test the feasibility of protein degradation on chip. To this end, wt and
400 non-degradable variants of Flag-Securin-GFP as well as Flag-p27-GFP (IVT products) were
401 loaded on the chip and captured in protein chambers along separate channels. All proteins
402 were immobilized via biotinylated anti-GFP antibodies. After washing, NDB mitotic extracts
403 were loaded into the extract chamber and trapped by closing the neck valve. Untrapped
404 materials were washed away. The device was heated to 30°C and scanned to obtain signals of
405 t_0 . The opening of the neck valve initiated degradation reactions in all cell units

406 simultaneously (Figure 5A and B), and the chip was scanned in time intervals of 20 min.
407 While the fluorescent signal of non-degradable Securin and p27 remained stable in NDB
408 mitotic extracts throughout the experiment, the signal of Flag-Securin-GFP diminished with
409 time (Figure 5C), revealing the regulated proteolysis of this protein in anaphase.

410

411 **Discussion**

412 pDOC is a lab-on-chip platform devised to facilitate and simplify discovery and
413 analysis of protein degradation in physiologically relevant contexts. The chip accommodates
414 hundreds of microchambers in which protein degradation can be assayed promptly and
415 simultaneously using considerably lower quantities of reagents compared to conventional
416 assays. The latter feature is especially crucial for the cell-free extracts whose production can
417 be a bottleneck in terms of time, activity, and amount. Signal detection on pDOC is based on
418 in situ quantification of fluorescent signal. The method is independent of contaminating
419 radioactive materials and yet, with sensitivity that surpasses traditional assays. A comparison
420 between pDOC and the conventional degradation assay is illustrated in Figure 6.

421 The flexibility of pDOC is significant; the platform facilitates almost all possible
422 experimental designs. First, both tagged and untagged proteins can be assayed, with detection
423 based on incorporation of Green-Lys, fluorescent proteins, or immunodetectable tags.
424 Second, pDOC can be used as an integrated microfluidics column for instant analyses of off-
425 chip degradation reaction. Alternatively, protein degradation can be assayed entirely on-chip
426 and in real time. Third, pDOC allows high-throughput experiments, in which the same
427 protein is tested for degradation in multiple extract/reaction solutions, or the same extracts
428 are applied to dozens of different proteins, simultaneously. Finally and importantly, pDOC is
429 inherently compatible with on-chip in vitro translation [24, 25, 27]. By expressing array of
430 proteins on-chip, one can multiplex the protein targets from tens to thousands, increasing

431 throughput dramatically. The downside of on-chip expression is that the assembly of the
432 device with the DNA microarray is not trivial and currently has to be performed by experts in
433 specialized laboratories.

434 Ubiquitin-mediated proteolysis is routinely assayed in hundreds of research
435 laboratories worldwide. We devised pDOC to facilitate and simplify in vitro analyses of
436 protein degradation. The method is fast, sensitive, reagent-saving, cost-effective, and
437 inherently optimal for both low- and high-throughput studies. It is also noteworthy that full
438 automation of the platform is foreseeable. We therefore believe that pDOC holds a great
439 potential in basic and translational research.

440

441 **Acknowledgements**

442 We thank the Gerber and Tzur lab members for sharing reagents. The Tzur lab is
443 supported by the Israel Science Foundation (ISF) Grant no. 2038/19.

444

445 **The authors declare no competing interests**

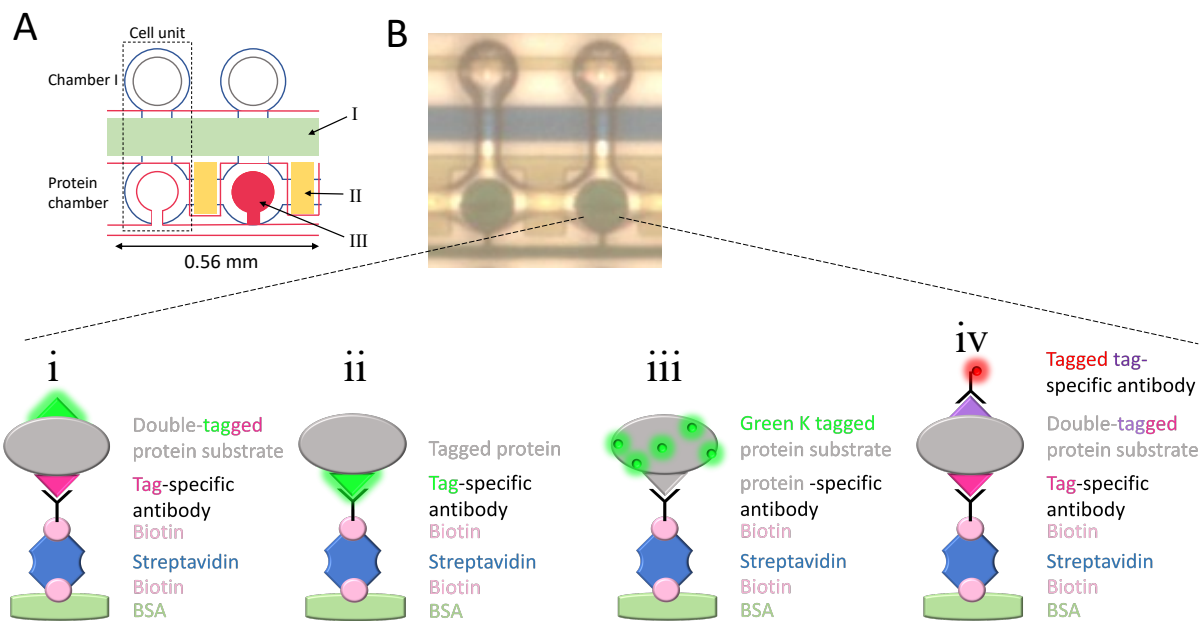
446 **References**

- 447 1. Ruz C, Alcantud JL, Montero FV, et al (2020) Proteotoxicity and neurodegenerative
448 diseases. *Int. J. Mol. Sci.* 21:1–25
- 449 2. Ciechanover A (2005) Proteolysis: From the lysosome to ubiquitin and the
450 proteasome. *Nat. Rev. Mol. Cell Biol.* 6:79–86
- 451 3. Emanuele MJ, Enrico TP, Mouery RD, et al (2020) Complex Cartography: Regulation
452 of E2F Transcription Factors by Cyclin F and Ubiquitin. *Trends Cell Biol.* 0
- 453 4. Skaar JR, Pagano M (2009) Control of cell growth by the SCF and APC/C ubiquitin
454 ligases. *Curr Opin Cell Biol* 21:816–824. <https://doi.org/10.1016/j.ceb.2009.08.004>
- 455 5. Peters JM (1998) SCF and APC: the Yin and Yang of cell cycle regulated proteolysis.
456 *Curr Opin Cell Biol* 10:759–68
- 457 6. Fuchs SY, Spiegelman VS, Kumar KGS (2004) The many faces of β -TrCP E3
458 ubiquitin ligases: Reflections in the magic mirror of cancer. *Oncogene* 23:2028–2036
- 459 7. Zur A, Brandeis M (2002) Timing of APC/C substrate degradation is determined by
460 fzy/fzr specificity of destruction boxes. *EMBO J* 21:4500–10.
461 <https://doi.org/10.1093/emboj/cdf452>
- 462 8. Skaar JR, Pagan JK, Pagano M (2013) Mechanisms and function of substrate
463 recruitment by F-box proteins. *Nat. Rev. Mol. Cell Biol.* 14:369–381
- 464 9. Kernan J, Bonacci T, Emanuele MJ (2018) Who guards the guardian? Mechanisms
465 that restrain APC/C during the cell cycle. *Biochim. Biophys. Acta - Mol. Cell Res.*
466 1865:1924–1933
- 467 10. Choudhury R, Bonacci T, Arceci A, et al (2016) APC/C and SCF(cyclin F) Constitute
468 a Reciprocal Feedback Circuit Controlling S-Phase Entry. *Cell Rep* 16:3359–3372.
469 <https://doi.org/10.1016/j.celrep.2016.08.058>
- 470 11. Kaiser P, Flick K, Wittenberg C, Reed SI (2000) Regulation of transcription by
471 ubiquitination without proteolysis: Cdc34/SCF(Met30)-mediated inactivation of the
472 transcription factor Met4. *Cell* 102:303–314. [https://doi.org/10.1016/S0092-](https://doi.org/10.1016/S0092-8674(00)00036-2)
473 [8674\(00\)00036-2](https://doi.org/10.1016/S0092-8674(00)00036-2)
- 474 12. Bonacci T, Emanuele MJ (2020) Dissenting degradation: Deubiquitinases in cell cycle
475 and cancer. *Semin Cancer Biol* 67:145–158.
476 <https://doi.org/10.1016/j.semcancer.2020.03.008>
- 477 13. Erales J, Coffino P (2014) Ubiquitin-independent proteasomal degradation. *Biochim.*
478 *Biophys. Acta - Mol. Cell Res.* 1843:216–221

- 479 14. Glotzer M, Murray AW, Kirschner MW (1991) Cyclin is degraded by the ubiquitin
480 pathway. *Nature* 349:132–138. <https://doi.org/10.1038/349132a0>
- 481 15. Murray AW, Solomon MJ, Kirschner MW (1989) The role of cyclin synthesis and
482 degradation in the control of maturation promoting factor activity. *Nature* 339:280–
483 286. <https://doi.org/10.1038/339280a0>
- 484 16. Ayad NG, Rankin S, Ooi D, et al (2005) Identification of ubiquitin ligase substrates by
485 in vitro expression cloning. *Methods Enzymol.* 399:404–414
- 486 17. Nguyen PA, Groen AC, Loose M, et al (2014) Spatial organization of cytokinesis
487 signaling reconstituted in a cell-free system. *Science* (80-) 346:244–247.
488 <https://doi.org/10.1126/science.1256773>
- 489 18. Wasserman D, Nachum S, Cohen M, et al (2020) Cell cycle oscillators underlying
490 orderly proteolysis of E2F8. *Mol Biol Cell* mbcE19120725.
491 <https://doi.org/10.1091/mbc.E19-12-0725>
- 492 19. Rape M, Kirschner MW (2004) Autonomous regulation of the anaphase-promoting
493 complex couples mitosis to S-phase entry. *Nature* 432:588–595.
494 <https://doi.org/10.1038/nature03023>
- 495 20. Yamano H, Gannon J, Mahbubani H, Hunt T (2004) Cell Cycle-Regulated
496 Recognition of the Destruction Box of Cyclin B by the APC/C in *Xenopus* Egg
497 Extracts. *Mol Cell* 13:137–147. [https://doi.org/10.1016/S1097-2765\(03\)00480-5](https://doi.org/10.1016/S1097-2765(03)00480-5)
- 498 21. Wang W, Wu T, Kirschner MW (2014) The master cell cycle regulator APC-Cdc20
499 regulates ciliary length and disassembly of the primary cilium. *Elife* 3:e03083.
500 <https://doi.org/10.7554/eLife.03083>
- 501 22. Khan OM, Almagro J, Nelson JK, et al (2021) Proteasomal degradation of the tumour
502 suppressor FBW7 requires branched ubiquitylation by TRIP12. *Nat Commun* 12:.
503 <https://doi.org/10.1038/s41467-021-22319-5>
- 504 23. Meyer HJ, Rape M (2014) Enhanced protein degradation by branched ubiquitin chains.
505 *Cell* 157:910–921. <https://doi.org/10.1016/j.cell.2014.03.037>
- 506 24. Gerber D, Maerkl SJ, Quake SR (2009) An in vitro microfluidic approach to
507 generating protein-interaction networks. *Nat Methods* 6:71–74.
508 <https://doi.org/10.1038/nmeth.1289>
- 509 25. Glick Y, Ben-Ari Y, Drayman N, et al (2016) Pathogen receptor discovery with a
510 microfluidic human membrane protein array. *Proc Natl Acad Sci U S A* 113:4344–
511 4349. <https://doi.org/10.1073/pnas.1518698113>
- 512 26. Glick Y, Avrahami D, Michaely E, Gerber D (2012) High-throughput protein

- 513 expression generator using a microfluidic platform. *J Vis Exp*.
514 <https://doi.org/10.3791/3849>
- 515 27. Noach-Hirsh M, Nevenzal H, Glick Y, et al (2015) Integrated microfluidics for protein
516 modification discovery. *Mol Cell Proteomics* 14:2824–2832.
517 <https://doi.org/10.1074/mcp.M115.053512>
- 518 28. Nevenzal H, Noach-Hirsh M, Skornik-Bustan O, et al (2019) A high-throughput
519 integrated microfluidics method enables tyrosine autophosphorylation discovery.
520 *Commun Biol* 2:1–8. <https://doi.org/10.1038/s42003-019-0286-9>
- 521 29. Ben-Ari Y, Glick Y, Kipper S, et al (2013) Microfluidic large scale integration of
522 viral-host interaction analysis. *Lab Chip* 13:2202–2209
- 523 30. Chen D, Orenstein Y, Golodnitsky R, et al (2016) SELMAP - SELEX affinity
524 landscape MAPPING of transcription factor binding sites using integrated
525 microfluidics. *Sci Rep* 6:. <https://doi.org/10.1038/srep33351>
- 526 31. Wasserman D, Nachum S, Noach-Hirsh M, et al (2021) Elucidating Human Using an
527 Anaphase-Like Cell-Free System. In: *Methods in molecular biology* (Clifton, N.J.).
528 *Methods Mol Biol*, pp 143–164
- 529 32. Maerkl SJ, Quake SR (2007) A systems approach to measuring the binding energy
530 landscapes of transcription factors. *Science* (80-) 315:233–237.
531 <https://doi.org/10.1126/science.1131007>
- 532 33. Glick Y, Orenstein Y, Chen D, et al (2015) Integrated microfluidic approach for
533 quantitative high-throughput measurements of transcription factor binding affinities.
534 *Nucleic Acids Res* 44:51. <https://doi.org/10.1093/nar/gkv1327>
- 535 34. Pe'er T, Lahmi R, Sharaby Y, et al (2013) Gas2l3, a Novel Constriction Site-
536 Associated Protein Whose Regulation Is Mediated by the APC/CCdh1 Complex. *PLoS*
537 *One* 8:. <https://doi.org/10.1371/journal.pone.0057532>
- 538 35. Carrano AC, Eytan E, Hershko A, Pagano M (1999) SKP2 is required for ubiquitin-
539 mediated degradation of the CDK inhibitor p27. *Nat Cell Biol* 1:193–199.
540 <https://doi.org/10.1038/12013>
- 541 36. Meyer HJ, Rape M (2011) Processive ubiquitin chain formation by the anaphase-
542 promoting complex. *Semin. Cell Dev. Biol.* 22:544–550
- 543 37. Lu Y, Lee BH, King RW, et al (2015) Substrate degradation by the proteasome: A
544 single-molecule kinetic analysis. *Science* (80-) 348:.
545 <https://doi.org/10.1126/science.1250834>
- 546
547

548 **Figures and figure legends**



549

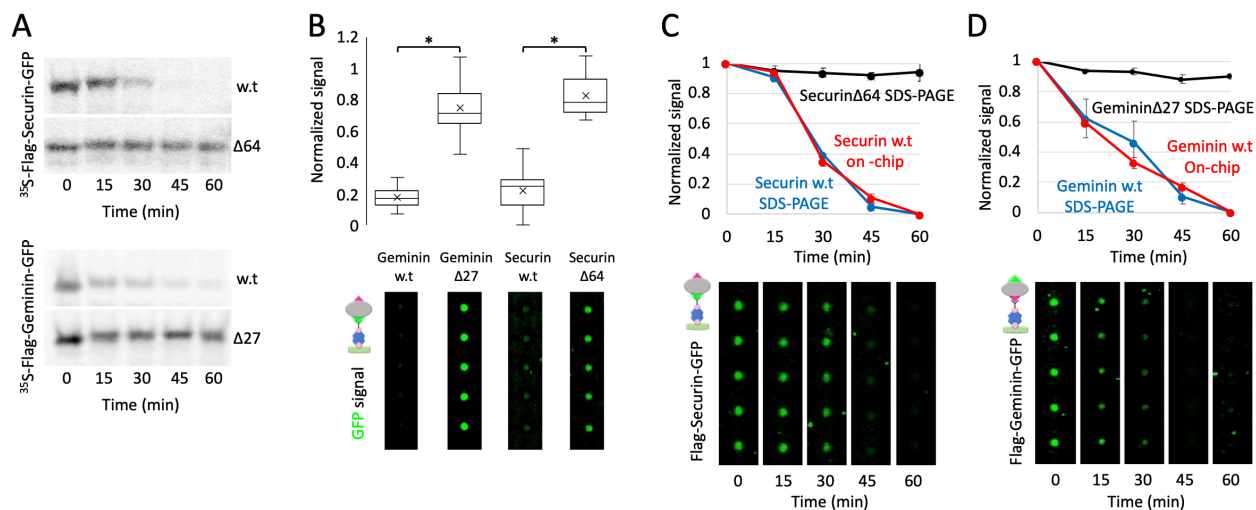
550 **Figure 1: The pDOC device, surface chemistry and detection of target proteins.** (A) An illustration of two
 551 cell units within MITOMI-based chip. Each cell unit (see black frame) comprises two chambers controlled by
 552 three pneumatic integrated valves. The two chambers are separated by the ‘neck valve’ (I). Different cell units
 553 are separated via sandwich valves (II). Samples containing target proteins (IVT products) are loaded into the
 554 protein chamber and immobilized via biotinylated antibodies that can be either protein- or tag specific. The
 555 target proteins are trapped via the MITOMI button valve (III) for quantification while the remaining unbound
 556 biomaterials are washed away. (B) Target proteins can be immobilized and quantified in several ways
 557 (illustrated): i) An example of a target protein carrying a fluorescent tag (e.g., GFP) for detection (see green
 558 glowing tag) and a non-fluorescent tag for immobilization; ii) A target protein tagged with GFP for both
 559 immobilization (by anti-GFP antibodies) and detection; iii) The target protein is untagged. Detection is based on
 560 fluorescent Lysine (Lys) incorporated during in vitro translation. Immobilization is via protein-specific
 561 antibodies. iv) The target protein is immobilized via tag- or protein-specific antibodies and detected by
 562 immunofluorescence via tag-specific antibodies coupled to fluorophore. Overall, on-chip immobilization of
 563 target proteins relies on biotinylated antibodies. Immobilization via non-biotinylated antibodies is possible if
 564 surface chemistry includes biotinylated IgG.

565

566

567

568



569

570

571

572

573

574

575

576

577

578

579

580

581

582

583

584

585

586

587

588

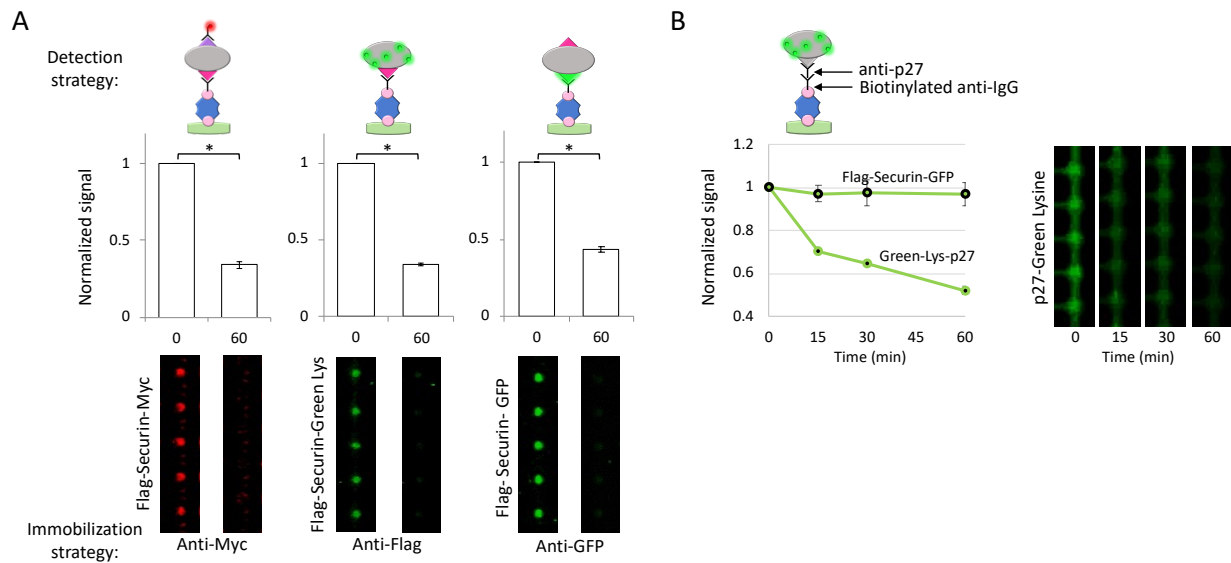
589

590

591

592

Figure 2. On-chip analysis of protein degradation assays. (A) Time-dependent degradation of ^{35}S -labeled Flag-Securin-GFP, Flag-Geminin-GFP and their non-degradable variants ($\Delta 64$ and $\Delta 27$, respectively) in NDB mitotic extracts supplemented with E-mix and Ubiquitin. Time-dependent proteolysis was resolved by SDS-PAGE and autoradiography. **(B)** Equivalent assays were performed with non-radioactive IVT products. Target proteins were incubated 1 h in reaction solution containing either extracts or PBS (control). Aliquots of each reaction mix (5 μl) were then loaded directly on a chip via separate channels, each containing dozens of cell units. Target proteins were immobilized to protein chambers via biotinylated anti-GFP antibody. The GFP tag was also used for quantification. GFP signals were calculated from 25-30 cell units per target protein per reaction condition (extracts vs. PBS). Box plots depict ratios of GFP signals (extracts/PBS) at $t_{60 \text{ min}}$. Mean (x) and median (-) are indicated. * p value <0.001. Representative raw data depicting detection on chip of the four target proteins are shown. **(C)** The degradation of Flag-Securin-GFP variant was assayed in tube as described in B. Here, however, aliquots were snap-frozen every 15 min. Time-lapse samples were then loaded on the chip for analysis. Target proteins were immobilized in protein chambers via anti-GFP antibodies and quantified based on GFP fluorescence. Time-dependent degradations of w.t vs. mutant Securin were quantified based on ^{35}S signal (standard analysis; $N=3$) and GFP fluorescence (on-chip analysis). Plots depict mean signals and standard error bars. Signals were normalized between max (1, t_0) and min (0, $t_{60 \text{ min}}$) values, allowing proper comparison between two very different methods of detection. **(D)** Equivalent experiment to (C) performed with Flag-Geminin-GFP, except that immobilization was based on anti-Flag antibodies.



594

595

596

597

598

599

600

601

602

603

604

605

606

607

608

609

610

611

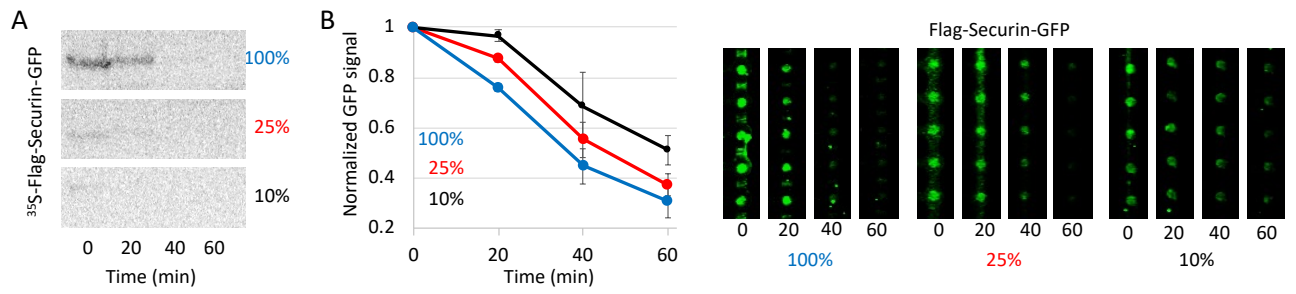
612

613

614

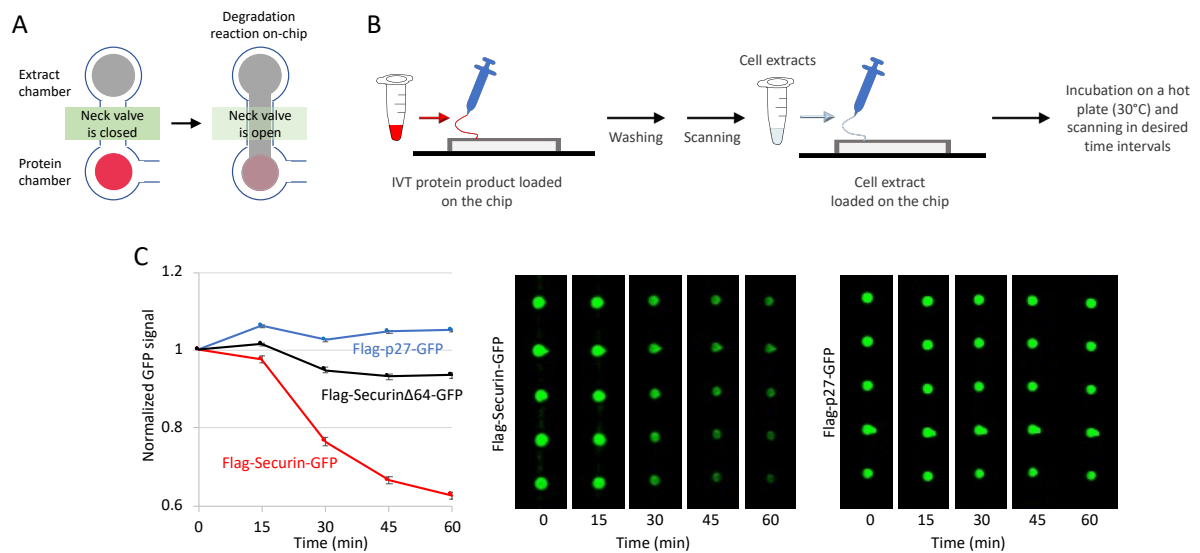
615

Figure 3. Method versatility. (A) Degradation of Flag-Securin-Myc, Flag-Securin-GFP, and Green-Lys-labeled Flag-Securin (IVT products) in NDB mitotic extracts was assayed in tube for 1 h. On-chip analysis was performed in multiple ways: 1) Flag-Securin-Myc was immobilized by anti-Myc antibodies and detected by anti-Flag Cy5-conjugated antibodies; 2) Flag-Securin-GFP was immobilized and detected via the GFP tag; and 3) Green-Lys-labeled Flag-Securin was immobilized via anti-Flag antibodies and detected by the Green-Lys signal. Anti-Myc/Flag/GFP antibodies are biotinylated. Plots and raw data depict protein levels at t_0 vs. $t_{60 \text{ min}}$. Signals are normalized to max values at t_0 . Mean values and standard error bars are shown; $20 < N < 30$ cell units. * p value < 0.001 . (B) Degradation of Green-Lys-labeled p27 (untagged) and Flag-Securin-GFP was assayed in S-phase extracts and analyzed by pDOC. p27 was immobilized via biotinylated anti-mouse IgG and anti-p27 antibodies and detected by Green-Lys. Flag-Securin-GFP was immobilized via biotinylated anti-Flag antibodies. Following incubation with cell extracts, protein levels were quantified by GFP or Green-Lys fluorescence in 15 min intervals. Plots depict mean and standard error values normalized to max signal at t_0 . $N = 25$ cell units.



616
 617
 618
 619
 620
 621
 622
 623
 624

Figure 4: Method sensitivity. (A) Time-dependent degradation assay of ³⁵S-labeled Flag-Securin-GFP in NDB mitotic extracts. Assays were performed with undiluted IVT product (100%) or following 4x/10x dilution in reticulocyte lysate (25% and 10%, respectively). In all assays, 1 μl substrate was incubated in 20 μl cell extracts. Samples were snap-frozen in 20 min intervals and assayed by SDS-PAGE and autoradiography. **(B)** Equivalent degradation assays performed with non-radioactive Flag-Securin-GFP. Time-point samples were loaded on the chip for immobilization (via anti-GFP-biotinylated antibody) and detection (GFP fluorescence). The plots summarize data from three experiments, 25 cell unites per experiment. Normalized mean and standard error values are shown (left). Representative raw data are shown on the right.



625

626

627

628

629

630

631

632

633

634

635

636

637

638

639

640

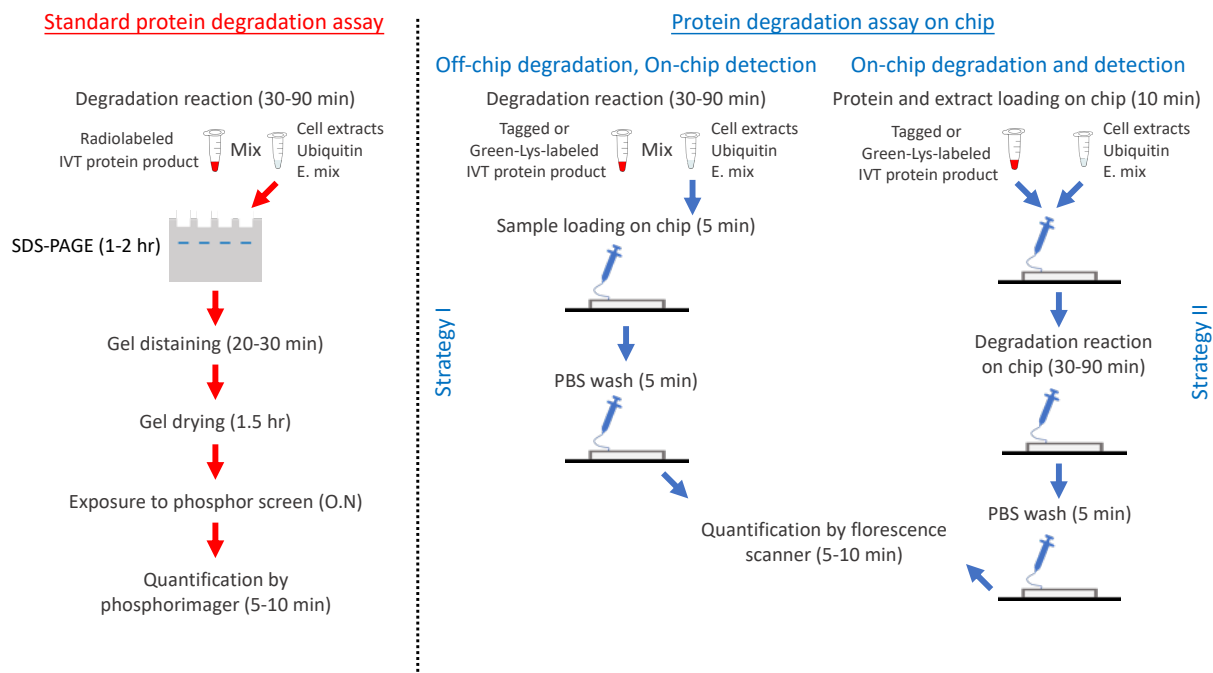
641

642

643

644

Figure 5: Protein degradation on chip. (A and B) Schematic illustration of complete on-chip degradation assay. IVT protein products are immobilized to the surface of the ‘protein chamber’ via biotinylated antibodies (see more information in Figure 1). The closing of the button valve traps the protein. All remains are washed away with PBS. Proper expression and immobilization of the target proteins are validated by scanning. Next, cell-free extracts are loaded into chamber I, i.e., ‘extract chamber’. The reaction begins with the opening of the neck valve and the diffusion of cell extracts into the ‘protein chamber’. The chip is placed on a 30°C hot plate and scanned at desired time intervals to provide kinetic information in real time. (C) GFP-tagged Securin and p27 IVT products were immobilized via anti-GFP-biotinylated antibody. Extract chambers were then filled with NDB mitotic extracts that support ubiquitination of Securin, but not of its non-degradable variant (Δ 64) and p27 (negative control validating assay specificity). Protein degradation was assayed for 1 hr during which the chip was scanned five times. The plot depicts mean GFP signals normalized to t_0 and standard error bars; $N=14-25$ cell units. Representative raw data for p27 and Securin are shown on the right.



646

647 **Figure 6: Schematic illustration of standard vs. two on-chip assays for protein degradation.** The purpose of all methods
 648 is to assay ubiquitin-mediated degradation of in vitro translated (IVT) proteins in cell-free systems comprising native cell
 649 extracts, extra ubiquitin and energy-regeneration mixture (E. mix). The standard assay (red pipeline) is typically radioactive.
 650 An ^{35}S -labeled IVT product (1-2 μl) is mixed with 20-50 μl reaction mixture, and incubated for 30-90 min. Each time point
 651 an aliquot ($\sim 5 \mu\text{l}$) of the reaction mix is harvested. Samples are denatured and resolved by SDS-PAGE. Following drying,
 652 the gel is exposed to a phosphor screen. Typically, a satisfactory signal is obtained overnight (O.N). Longer exposures (24-
 653 72 hrs) are often needed when the radioactive signal is low due to a variety of reasons. Integrated microfluidics provides two
 654 alternative assays, both with significant benefits. Strategy I: The protein degradation is be assayed off-chip. The assay,
 655 however, is non-radioactive; the target protein is either fused to a standard tag (e.g., GFP, Flag, Myc, etc.) or translated in
 656 the presence of Green-Lys. Time-point samples are either loaded on the chip sequentially or harvested first (boil/snap-
 657 freeze) and then loaded simultaneously at the end of the reaction. The target protein is immobilized by tag/protein-specific
 658 surface antibodies, all other materials are washed away, and quantification is carried out by one of the strategies detailed in
 659 Figure 1B. Strategy II: Here, target proteins and cell extracts are loaded on the chip successively and occupy the protein and
 660 extract chambers, respectively. The mixing of the two materials (controlled by the neck valve; Figure 1B) initiates the
 661 reaction. Time-lapse scanning provides kinetic information. While Strategy I is simpler, Strategy II is more optimal for high-
 662 throughput assays. Both on-chip methods, however, are reagent-saving and considerably shorter than the standard assay.

663

664

665

666

667
668
669
670
671
672
673
674
675
676
677
678
679
680
681
682
683
684
685
686
687
688
689
690
691
692
693
694
695
696
697
698
699
700
701

Supplementary information

for

Protein degradation analysis by affinity microfluidics

Lev Brio^{1,2}, Danit Wasserman^{1,2}, Efrat Michaely-Barbiro¹, Doron Gerber^{1,3,*}, and Amit

Tzur^{1,3,*}

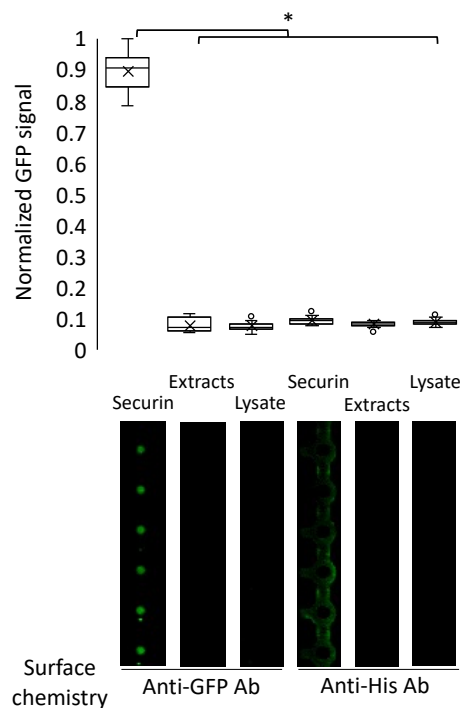
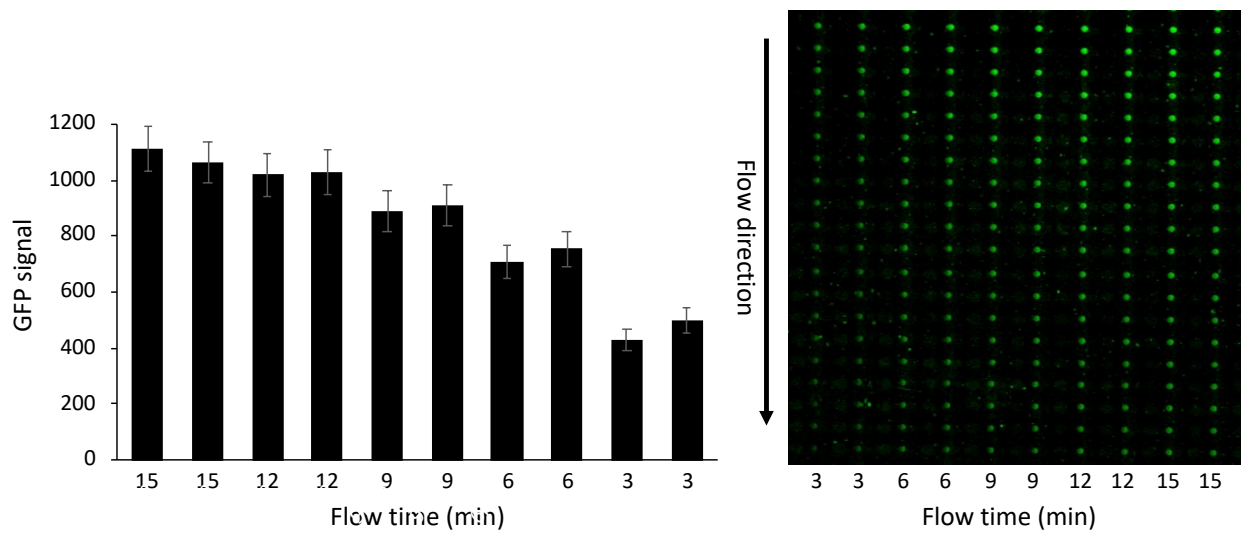


Figure 1S. Estimating background and noise signals on chip. An IVT product of Securin-GFP was loaded on a chip, immobilized to protein chambers via biotinylated anti-GFP antibodies, and mixed (on chip) with NDB mitotic extracts (see more information in figures 1 and 6). The GFP signal of the protein was immediately measured. Control experiments performed with 1) NDB mitotic extracts without Securin-GFP (Extracts) to measure the 488 nm-excited autofluorescence of the extracts; and 2) NDB mitotic extracts with reticulocyte lysate to measure the contribution of the lysate to the overall signal of the target protein. A similar set of experiments performed following surface chemistry with biotinylated anti-His antibodies to measure the contribution of non-specific protein interactions to the overall signal coming from the protein chamber. Box plot depicts mean (x) and median (-) signals normalized to maximum level. $N=39$; * p value <0.01 .

702



703

704

705

706

707

708

709

710

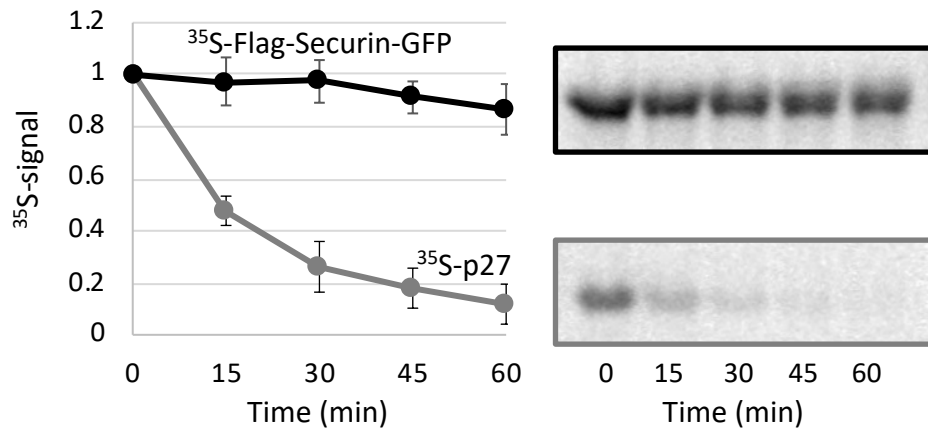
711

712

713

714

Figure 2S. Validating unsaturated signal detection by pDOC. 1 μ l IVT product of non-degradable (Δ 64) Flag-Securin-GFP was mixed with 20 μ l NDB mitotic extracts, following the volume ratio of a standard degradation reaction. Samples were immediately flown on the pDOC device for various time periods (depicted) via separate channels (two channels per sample). Flag-Securin-GFP was immobilized to protein chambers via biotinylated anti-GFP antibodies and detected by GFP fluorescence. The plot depicts mean values calculated from 20 cell units (arbitrary units). Throughout this study, reaction samples were flown for 3-5 min to avoid any risk of signal saturation. To clarify, per experiment the flow time of all samples is identical. Raw data are shown on the right.



715
716
717
718
719
720
721
722
723
724
725

Figure S3. Conventional degradation assay of p27. During DNA synthesis (S) phase, p27 is ubiquitinated by the SCF^{Skp2} E3 complex and degraded whereas Securin remain stable. ³⁵S-labeled IVT products of both proteins were incubated in human cell-free system recapitulating S-phase. Protein degradation was assayed by SDS-PAGE and autoradiography (standard protocol). p27, but not Securin, was degraded in this condition. Quantifications and representative raw data are shown. The plot depicts mean and standard error values; *N*=3.



726
727
728
729
730

Figure S4. An estimation of Securin concentration in reticulocyte lysate following translation. Various amounts of recombinant His-Securin [34] and 1 µl of three Flag-Securin-GFP IVT products were resolved on SDS-PAGE for Western blot analysis with anti-Securin antibody. The estimated concentration of Flag-Securin-GFP IVT product is 400 nM.